Appl Magn Reson (2013) 44:247–265
DOI 10.1007/s00723-012-0395-9

Applied
Magnetic Resonance

NMR Studies of the Reaction Path of the *o*-H_2/*p*-H_2 Spin Conversion Catalyzed by Vaska's Complex in the Solid State

Jochen Matthes · Stephan Gründemann · Gerd Buntkowsky · Bruno Chaudret · Hans Heinrich Limbach

Received: 10 July 2012 / Published online: 16 October 2012

Abstract We have studied the *o*/*p* spin conversion of dihydrogen in contact with frozen solutions of Vaska's complex $Ir(CO)Cl(PPh_3)_2$ (**1**) in C_6D_6 and with polycrystalline **1** at 77 K. The main purpose of this study was to elucidate the mechanism of this type of reactions found accidentally previously (Eisenschmid et al JACS 109:8089–8091, 1987 and Eisenberg ACS 24:110–116, 1991). The formation of *p*-H_2 was followed after thawing of the samples by ^1H nuclear magnetic resonance (NMR) spectroscopy at 298 K, where the oxidative addition of dihydrogen to **1** occurs leading to Vaska's dihydride $Ir(CO)ClH_2(PPh_3)_2$ (**2**) which is known to exhibit *para*-hydrogen-induced polarization (PHIP). The PHIP signal was shown to be proportional to the concentration of *p*-H_2 as elucidated from the decrease of the signal of dissolved *o*-H_2. The reaction was found to be faster for the frozen solution as compared to the polycrystalline powder. Optical microscopy showed that small particles of **1** are separated from the solution during the freezing process, exhibiting a larger surface area as compared to the polycrystalline powder. When a mixture of H_2 and D_2 was exposed to the frozen solutions or to the polycrystalline powder, the formation of HD was observed by ^1H NMR. This finding indicates the

Dedicated to Professor Hans-Martin Vieth on the occasion of his 70th birthday.

J. Matthes · S. Gründemann · H. H. Limbach (✉)
Institut für Chemie und Biochemie, Freie Universität Berlin,
Takustr. 3, 14195 Berlin, Germany
e-mail: limbach@chemie.fu-berlin.de

G. Buntkowsky
Eduard-Zintl-Institut für Anorganische und Physikalische Chemie,
Technische Universität, Darmstadt, Germany

B. Chaudret
Laboratoire de Physique et Chimie des Nano-Objets,
Institut National de Recherche Appliqué, Université de Toulouse,
31077 Toulouse, France

presence of a chemical spin conversion involving two dihydrogen molecules. Additional ^{1}H NMR experiments of dihydrogen in frozen C_6D_6 at 110 K indicated the formation of larger pores containing gaseous H_2 as well as dihydrogen sites in interstitial sites between benzene molecules. Moreover, in the presence of **1**, a signal at −4.5 ppm was observed which was attributed to a dihydrogen in close contact with Ir.

1 Introduction

About a quarter of a century ago, Eisenschmid et al. and Eisenberg [1, 2] discovered accidentally that it is possible to transfer nuclear polarization from hydrogen gas enriched with the *para*-nuclear spin isomer $H^{\uparrow}$–$H^{\downarrow}$ to unsaturated organic molecules via hydrogenation catalyzed by organometallic transition metal complexes in solution.

$$H^{\uparrow}-H^{\downarrow} + R_2C=CR_2 \rightarrow R_2CH^{\uparrow}-CH^{\downarrow}R_2 \text{ (PHIP)}. \quad (1)$$

The resulting enhanced sensitivity of the products for nuclear magnetic resonance (NMR) experiments has made *para*-hydrogen induced polarization (PHIP) an important tool with interesting potential applications in material sciences and medical imaging. In this study, we are concerned with the mechanisms leading to the initial discovery of PHIP.

It was earlier recognized by Weitekamp et al. [3] that PHIP depends on the magnetic field strength where the transfer takes place, i.e., under ALTADENA conditions at zero field, or under PASADENA conditions at high field. However, only recently Hans-Martin Vieth and his group [4] to whom this paper is dedicated, have studied the field-dependence in a systematic way, which is important for future applications. Bargon et al. [5] have demonstrated that it is possible to transfer the polarization from ^{1}H to heteronuclei which can exhibit longer longitudinal relaxation times and hence longer polarization times than ^{1}H. Recent advances are the possibility to create spin-polarized gases by reaction with solid catalysts [6, 7] and to transfer polarization to organometallic ligands without hydrogenation [8].

In our laboratory we have explored the pathways of the nuclear spin conversion of hydrogen spin isomers upon binding to transition metal centers [9–11]. During the binding process, the H···H distance increases and the energy difference, also called "exchange coupling", between the rotational *ortho*- and *para*-tunneling states decreases [12–16]. A magnetic spin conversion (SC) between *ortho*- and *para*-states (Eq. 2) can take place via a magnetic mechanism when the exchange couplings are of the order of the magnetic couplings [17].

$$H^{\uparrow}-H^{\uparrow} \leftrightarrows H^{\uparrow}-H^{\downarrow} \text{ (magnetic SC)}. \quad (2)$$

PHIP represents a special magnetic spin conversion case caused by different chemical shifts of the polarized nuclei in the hydrogenation products. By contrast, binding of two hydrogen molecules can lead to a chemical spin conversion (Eq. 3), in a similar way as the isotope scrambling (IS), i.e., HD production from H_2 and D_2 (Eq. 4)

$$H^{\uparrow}-H^{\uparrow} + H^{\downarrow}-H^{\downarrow} \leftrightarrows H^{\uparrow}-H^{\downarrow} + H^{\uparrow}-H^{\downarrow} \text{ (chemical SC)}, \quad (3)$$

$$H-H + D-D \leftrightarrows HD + HD \text{ (IS)}. \quad (4)$$

Within the framework of our mechanistic studies we have been interested what exactly happened during the accidental discovery of PHIP, which was commented by Eisenberg [2] as follows:

> But how did we come to a *para*-hydrogen-induced polarization when all we were studying was the reaction chemistry of metal hydride complexes with organic substrates? The answer, in retrospect, is simple. After samples were prepared during the day for NMR runs at night, they were stored in liquid N_2 baths at which temperature the only thing happening in the system was the slow conversion of *ortho* to *para* H_2 catalyzed by the frozen solution of the metal complex. By the time samples were thawed, a *para*-enriched-H_2 atmosphere had been generated, and upon shaking of the sample, reaction commenced with *para*-enriched H_2.

The main question which still remains is how a metal complex in a frozen solvent can catalyze the *ortho–para* spin conversion of hydrogen gas above the sample.

In order to address this problem we have performed experiments on the Vaska's [18, 19] catalyst $Ir(CO)Cl(PPh_3)_2$ (**1**). Frozen solutions of **1** at 77 K in benzene catalyze the conversion of the *o*-H_2 to -*p*-H_2 gas (Scheme 1a) as shown in a preliminary report [17] without alteration of the catalyst. By contrast, in liquid solution at room temperature **1** reacts within about 1 h with hydrogen to form Vaska's dihydride **2** (Scheme 1b). **2** shows PHIP signals if the reaction occurs with *para*-H_2 [17, 20, 21]. This feature can be used to detect *para*-H_2 formed in the sample during preparation. The dihydrogen complex **3** is probably an intermediate of the hydrogenation, but has not been observed directly up to date to our knowledge.

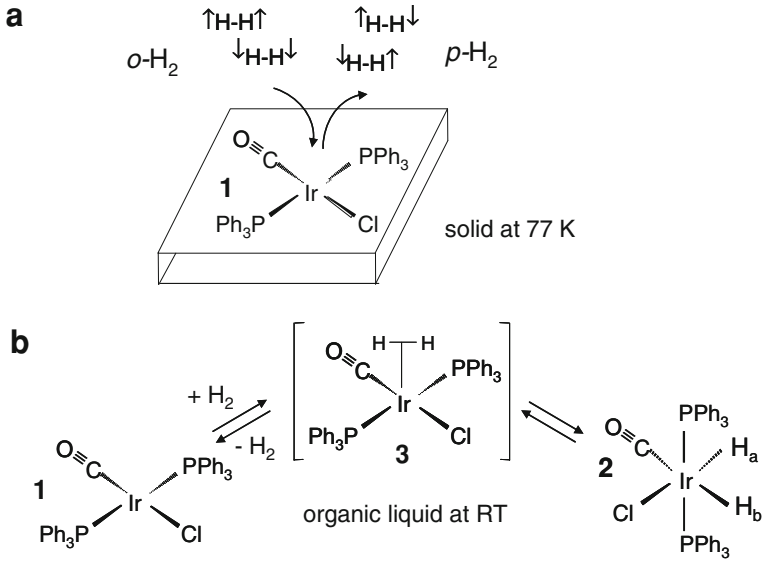

Scheme 1 Hydrogenic reactions of the Vaska's catalyst **1**

Here, we have followed the reaction of Scheme 1a in frozen benzene-d_6 directly by ^{1}H NMR spectroscopy as well as by optical microscopy of the reacting solid. For reference, we have also performed measurements of H_2 in frozen benzene-d_6 without catalyst. Our measurements allow us to decide whether the reacting solid constitutes a solid solution, or a heterogeneous solid, with different environments for H_2, which might constitute reaction intermediates.

This paper is organized as follows. After an experimental section the results are presented and discussed.

2 Experimental Procedure

2.1 ^{1}H NMR Experiments

The ^{1}H NMR spectra were recorded using a Bruker AMX 500 MHz spectrometer equipped with 5-mm probe which could be used down to about 100 K.

2.2 Preparation of NMR Samples

Vaska's complex $Ir(CO)Cl(PPh_3)_2$ **1** (99.9 %) and C_6D_6 were purchased from Sigma-Aldrich. NMR samples were prepared using the glass device depicted in Fig. 1 attached to a vacuum line. C_6D_6 was stored in a glass solvent container over Na/K alloy and degassed several times before use. A 5 mm J. Young NMR tube (Wilmad, Buena) was attached to the vacuum by a Teflon needle valve, which was part of the NMR tube. H_2 and D_2 gas were stored in metallic lecture bottles (Sigma-Aldrich) attached to the device. The gas pressure was gauged using a manometer. Different types of samples and experiments were performed as described in the next section. The concentration of standard samples of **1** in C_6D_6 was always 1 mg in 1 ml, i.e., 1.3×10^{-3} M.

3 Results

3.1 Oxidative Addition of Dihydrogen to Vaska's Complex **1** Followed by ^{1}H NMR

In a first step, a degassed saturated standard solution of **1** in dry C_6D_6 was prepared by vacuum transfer into the NMR tube (Fig. 1) cooled at the bottom to 77 K. Then, 800 mbar H_2 was let into the NMR tube by opening the appropriate valves. After rapid thawing at 300 K using a water bath, with all valves closed and carefully shaking the sample to obtain equilibration of H_2 between the liquid and the gas phase within the tube, the spectra depicted in Fig. 2 were taken which indicate the slow addition of dihydrogen to **1** leading to the dihydride **2** according to Scheme 1.

At 7.95 ppm we observe a broad signal for the *ortho*-hydrogens of the phosphine ligands of **1** being converted to a pseudo quartet at 7.91 ppm ($J_{HH} = 5.72$, 7.0 Hz, respectively) during the course of hydrogenation. The latter signal is assigned to the

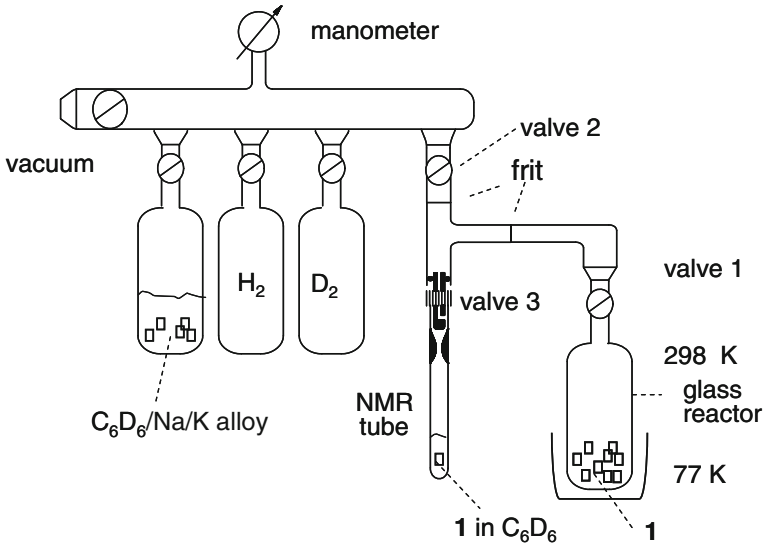

Fig. 1 Vacuum manifold used for sample preparation

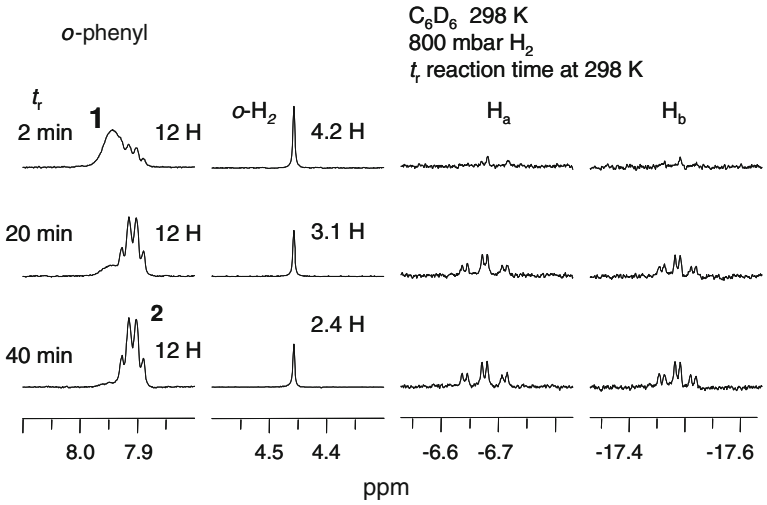

Fig. 2 ^{1}H NMR spectra at 298 K of a standard sample of **1** in C_6D_6 (1.3×10^{-3} M) under 800 mbar of H_2 at different times t_r of the reaction to **2**. The addition of H_2 was done at 77 K after which the sample was thawed to 298 K and shaken prior to the measurement. (500.13 MHz, 4 scans, 20 s pulse delay, $\pi/4$ pulses 3.5 μs)

ortho-hydrogen of the phosphine ligand in the product complex $IrH_2COCl(PPh_3)_2$ (**2**). The broad signal of the ligand might arise due to agostic interactions with the unsaturated metal center in **1** causing the rotation to slow down. In the 18e-complex **2** no agostic interaction can take place and the ligands can rotate freely around the Ir-P axes resulting in a sharp signal. The integral of the aromatic *o*-proton signals of

1 and **2** was set to the value of 12 H. As this number is constant during the reaction, the integrals of the other signals were referenced to this value. Thus, the signal intensities I used in this study are dimensionless. We estimate that the margin of error of these signal intensities is between 5 and 10 %. Dissolved free dihydrogen resonates in benzene at 4.45 ppm. Its initial intensity of 4.2 H decreases with time as H_2 is consumed during the reaction. This observation illustrates that no significant amount of dihydrogen enters the solution from the gas phase during the reaction, i.e., that the equilibration of H_2 between the gas- and the solution-phase is slow. At high field at −6.67 and at −17.49 ppm the signals of the two non-equivalent hydrides of **2** emerge slowly as the reaction proceeds. The signal patterns consist of triplets of doublets—due to coupling with the two equivalent phosphorus nuclei (J_{HP} = 17.5 and 14 Hz, respectively) and the coupling between the two hydrides with J_{HH} = 4.8 Hz [20].

An estimate of the reaction rate can be obtained as follows. The reaction of **1** dissolved at $c = 1.28 \times 10^{-3}$ mol l^{-1} in 1 ml of benzene with the double amount of H_2 (2.56×10^{-3} mol l^{-1}) takes 1 h (t = 3,600 s). We determined the H_2 concentration in 1 ml of benzene by signal integration of the NMR spectrum. The rate of the reaction is calculated to be $c/t = 3.56 \times 10^{-6}$ mol l^{-1} s^{-1}. The reaction constant k is calculated to $k = [\mathbf{1}]/(t[\mathbf{1}][H_2]) = 1.09 \times 10^{-5}$ (s mol)$^{-1}$ l, which is in good agreement with the result of Vaska, who found $k = 1.2 \times 10^{-5}$ (s mol)$^{-1}$ l [19].

This reaction of **1**–**2** in solution is slow and complete only after about 1 h, which corresponds to a bimolecular rate constant of about 10^{-5} l mol^{-1} s^{-1} [19]. An activation energy of 50 kJ mol^{-1} has been reported [22] and calculated by Hartree–Fock and Moller–Plesset perturbation theory to be about 55 kJ mol^{-1}. The reaction is slow because of the necessary ligand reorientation.

3.2 *Ortho–Para* H_2 Conversion in Frozen Solutions of Vaska's Complex in C_6D_6

As mentioned in the Sect. 1, we wanted to study whether and how the *ortho–para* H_2 conversion takes place in a frozen solution at low temperatures, exposed to gaseous dihydrogen at room temperature. Moreover, the question arose whether the oxidative addition of H_2 to **1** producing **2** (Scheme 1) takes place under these conditions. We thus prepared different standard samples of **1** in C_6D_6 (1.3×10^{-3} M) under 800 mbar H_2 in a similar way as described above; however, instead of measuring the ^{1}H NMR spectra after thawing and dissolution of **1** we froze each sample again rapidly to 77 K and stored it at that temperature for different exposure times t_{ex} to dihydrogen at 289 K, located in the gas phase above the cold solid. After thawing and carefully shaking the sample ^{1}H NMR spectra were taken at given time delays after thawing.

An example is shown in Fig. 3. In principle we obtain similar spectra as in Fig. 2, with the difference that now enhanced antiphase signals for the hydride sites of **2** are observed as has been described before [8], indicating the presence of an excess of *para*-H_2 which has been formed at 77 K, reacting now with **1** at a high magnetic field (PASADENA conditions). This PHIP effect is still visible after 30 min, however after 60 min it has disappeared, and the normal dihydride signals of **2** are

observed at −6.67 and −17.49 ppm, respectively. However, there is still a large amount of the precursor **1** present in the sample, as indicated by the aromatic proton signals. Thus, almost all dihydrogen has been consumed in the liquid. However, when the sample is carefully shaken, additional polarized dihydrogen in the gas phase dissolves again in the liquid phase indicated by the increased signal intensity at 4.46 ppm. Now, the reaction starts again and the PHIP effect is reproduced. However, as only the molecules formed in a small time period prior to the measurement exhibit the PHIP effect, the molecules formed in a previous reaction stage contribute the normal signals (Fig. 2); the overlap of both types of signals leads then to a smaller intensity of the left component of the two hydride doublets.

These results confirm the previous observation of Eisenberg et al. [1, 2] that *para*-H_2 is formed in frozen solutions of hydrogenation catalysts at 77 K when exposed to gaseous dihydrogen prior to the NMR measurement at room temperature, and that the PHIP signals are a measure of the concentration of *para*-H_2 in solution. In order to follow the *para*-H_2 production by analyzing the PHIP signals we measured, therefore, in the remaining experiments described in the following always under reproducible conditions, i.e., at 2 min after thawing and carefully shaking the samples.

Figure 4 presents spectra of three of the six samples differing in the storage times at 77 K. As we measured 2 min after thawing, the signals of the 12 *ortho*-phenyl protons of **1** resonating at 7.95 ppm remain unchanged, and only small amounts of

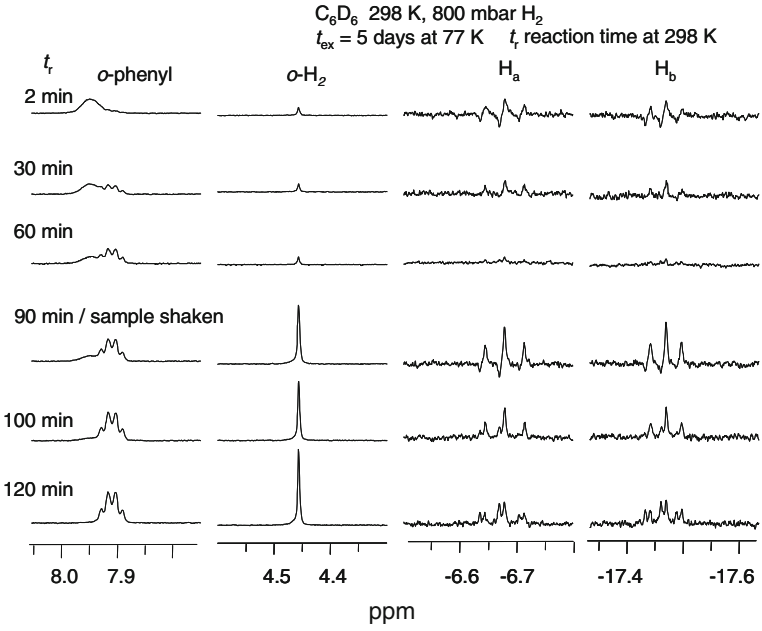

Fig. 3 ^{1}H NMR spectra at 298 K of a standard sample of **1** in C_6D_6 under 800 mbar of H_2 measured at different times t_r of the reaction to **2**. The sample was prepared in a similar way as the one of Fig. 2, but was exposed for the time $t_{ex} = 5$ days at 77 K to the warm dihydrogen gas prior to the measurement. (500.13 MHz, 4 scans, 20 s pulse delay, $\pi/4$ pulses 3.5 μs)

the corresponding protons of **2** have appeared. Therefore, the intensities of the other signals were referenced to these aromatic proton signals. By contrast, the signal intensity of o-H_2 is decreased, and the PHIP signal intensity of the hydride sites is increased. The data were analyzed in terms of the reversible pseudo-first order reaction

$$o\text{–}H_2 \underset{k_{po}}{\overset{k_{op}}{\leftrightarrows}} p\text{–}H_2, \tag{5}$$

where the evolution of the mole fractions of the two species as a function of time is given by:

$$\begin{aligned} x_{oH2} &= x^{\infty}_{oH2} + (x^{o}_{oH2} - x^{\infty}_{oH2})\exp(-kt), \\ x_{pH2} &= x^{\infty}_{pH2} + (x^{o}_{pH2} - x^{\infty}_{pH2})\exp(-kt). \end{aligned} \tag{6}$$

k is the sum of the forward and backward reaction rate constants

$$k = k_{op} + k_{po}. \tag{7}$$

The equilibrium mole fractions at 298 K are $x^{\infty}_{oH2} = 0.75$ and $x^{\infty}_{pH2} = 0.25$, which also constitute the initial mole fractions x^{o}_{oH2} and x^{o}_{pH2} at 77 K. The corresponding equilibrium mole fractions at 77 K are $x^{\infty}_{oH2} = x^{\infty}_{pH2} = 0.5$ [23], i.e., $k_{op} = k_{po}$. at 77 K. The mole fractions were obtained from the signal intensity of the dihydrogen signal at 4.45 ppm. As dihydrogen constitutes an A_2 spin system, the intensity of this signal is related to the mole fraction of o-H_2 and of p-H_2 by

$$x_{oH2} = x_H\left(x^{o}_{oH2} - \frac{3}{4}\frac{I^0_{H2} - I_{H2}}{I^0_{H2}}\right) = x_H\left(\frac{3}{4}\frac{I_{H2}}{I^0_{H2}}\right),\ x_{pH2} = 1 - x_{oH2}. \tag{8}$$

$x_H = 1 - x_D$ is the total H fraction, and x_D the deuterium fraction. In the present experiment $x_D = 0$, but the value was increased in subsequent experiments.

At the beginning of the reaction, the relative signal intensity of dissolved o-H_2 is $I_{H2} = I^0_{H2} = 4.2$, and drops after 10 days to a value of 2.94.

In Fig. 5a the mole fractions x_{oH2} and x_{pH2} of o-H_2 and p-H_2 calculated from the values of I_{H2} using Eq. (8) are plotted as a function of the time of the exposure of the frozen solution to 800 mbar of dihydrogen. We observe an exponential behavior as a function of time. From the fit of the data to Eq. (6) we obtain a pseudo-first order rate constant of $k = 0.35\ \text{day}^{-1}$. Figure 5b illustrates that the PHIP signal intensity I_{PHIP} exhibits a similar time dependence as x_{para}. Figure 5c shows that

$$I_{PHIP} = \text{const}(x_{pH2} - x^{\infty}_{pH2}),\ \text{const} = 4.5\ \text{day}^{-1}, \tag{9}$$

where $x^{\infty}_{pH2} = 0.25$ is now the value at room temperature. The constant is valid only for samples prepared and measured in a similar way.

3.3 Isotope Scrambling of H_2/D_2 Mixtures over Frozen Solutions of Vaska's Complex in C_6D_6 at 77 K

In order to distinguish between the magnetic o-H_2/p-H_2 conversion according to Eq. (2) involving a single dihydrogen molecule and the chemical mechanism of

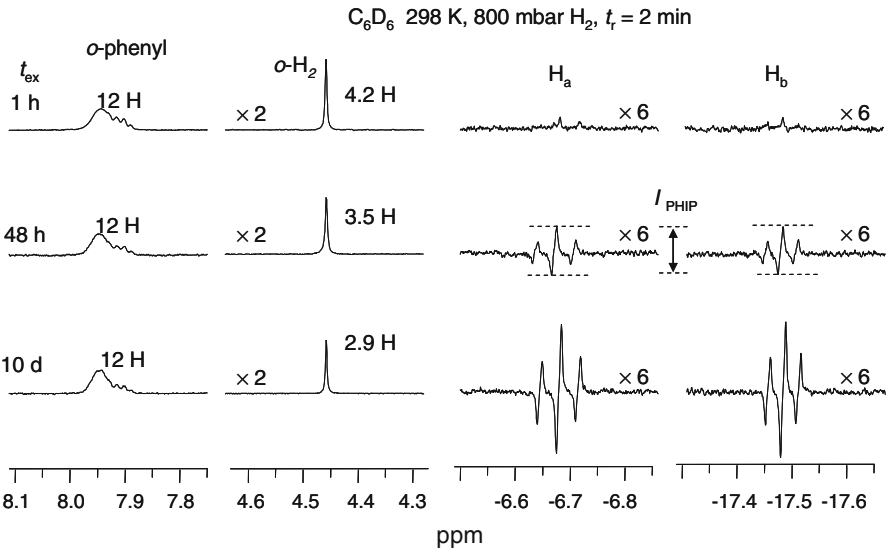

Fig. 4 ^{1}H NMR spectra at 298 K of standard samples of **1** in C_6D_6 under 800 mbar of H_2 measured at time $t_r = 2$ min of the reaction to **2**. The samples were prepared in a similar way as the one of Fig. 2, but were exposed for different times t_{ex} at 77 K to the warm dihydrogen gas prior to the measurement. (500.13 MHz, 4 scans, 20 s pulse delay, $\pi/4$ pulses 3.5 μs)

Eq. (3) involving the metathesis of two molecules, we have performed the following experiment. We let a 1:1 mixture of 400 mbar H_2 and of 400 mbar D_2 interact with a frozen standard solution of **1** in C_6D_6 (1 mg in 1 ml) at 77 K for 5 days. After thawing and carefully shaking the sample we obtained the spectrum illustrated in Fig. 6. At 4.5 ppm the signal of free dihydrogen is observed exhibiting an intensity of 0.76 with respect to the initial value of 2.1, and very closely at 4.42 ppm the well-known triplet of HD, caused by coupling with deuterium ($J_{HD} = 43$ Hz). The intensity of this signal was 0.18. In addition, p-H_2 is formed giving rise to PHIP of the high-field hydride signals of **2**.

The observation of HD formation at 77 K is very remarkable as it can only occur via the isotope scrambling reaction of Eq. (4),

$$H_2 + D_2 \underset{k_b}{\overset{k_f}{\leftrightarrows}} 2\ HD,\ K = \frac{k_f}{k_b}, \tag{10}$$

For a statistical distribution $K = 4$, whereas a value of 3.25 has been calculated using isotope theory [24] and has been confirmed experimentally [25] for 298 K.

As in this experiment $x_H = x_D = 1/2$, we have in case of a statistical distribution the initial values $x^o_{oH2} = 3/8,\ x^o_{pH2} = 1/8,\ x^0_{HD} = 0,\ x^0_{D2} = 1/2$, and at the end of the exposure period at 77 K the final values $x^\infty_{oH2} = x^\infty_{pH2} = 1/8,\ x^\infty_{HD} = 1/2,\ x^\infty_{D2} = 1/4$. As the mole fractions of o-H_2 and of HD are now given by

$$x_{oH2} = \frac{3}{8}\frac{I_{H2}}{I^0_{H2}} \text{ and } x_{HD} = \frac{I_{HD}}{I^0_{H_2}}, \tag{11}$$

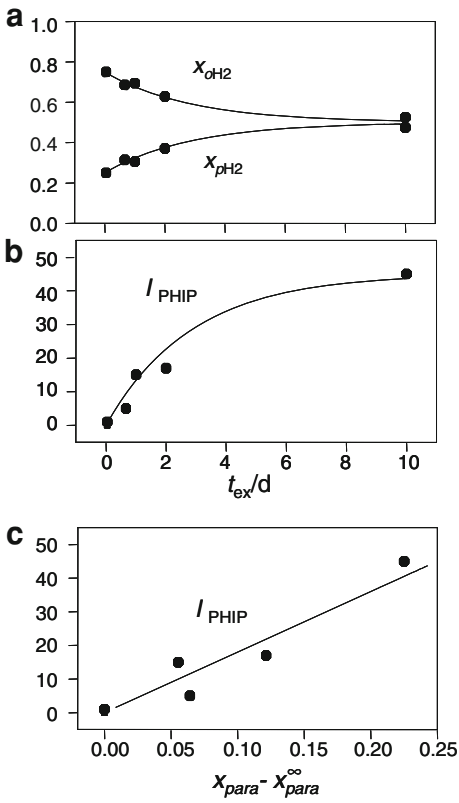

Fig. 5 **a** o-H_2 and p-H_2 mol fractions measured by analysis of the o-H_2 signal intensities I_{H2} (dimensionless) as a function of the exposure time t_{ex} in days at 77 K to 800 mbar of gaseous dihydrogen at 298 K. **b** Arbitrary PHIP signal intensities I_{PHIP} as a function of t_{ex}. **c** Correlation of I_{PHIP} with the mole fractions of p-H_2. The H_2 signal intensities $I_{H2} = 4.2$ H, 3.84 H, 3.89 H, 3.52 H, 2.94 H at $t_{ex} = 0.0417$, 0.083, 1, 2, and 10 days were referenced to the sum of the signals of the 12 *ortho*-phenyl protons of 1 and 2 set to a value of 12 H. The values I_{PHIP} were evaluated from the signal H_a and H_b as shown in Fig. 4, and are given by 1, 5, 15, 17, 45 in arbitrary units at $t = 0.0417$, 0.083, 1, 2, and 10 days. For further explanation see text

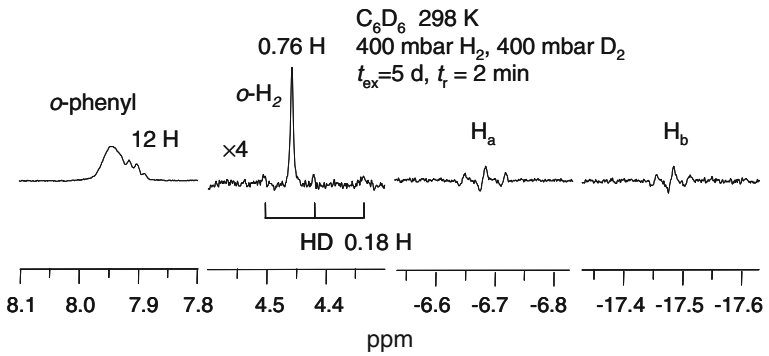

Fig. 6 ^{1}H NMR spectra at 298 K of a standard sample of **1** in C_6D_6 under a 1:1 mixture of 400 mbar H_2 and 400 mbar D_2 measured at time $t_r = 2$ min of the reaction to **2**. The sample was prepared in a similar way as the one of Fig. 2, but was exposed for time $t_{ex} = 5$ days at 77 K to the warm dihydrogen gas mixture prior to the measurement (500.13 MHz, 4 scans, 20 s pulse delay, $\pi/4$ pulses 3.5 μs)

it follows that the H_2 signal at 4.45 ppm will drop to 1/3 of its initial value, and the HD signal should rise to half of the initial H_2 signal intensity. This is almost fulfilled for the H_2 signal, with $I_{H2} = 0.76$ and $I^0_{H2} = 2.1$. However, the signal intensity of

$I_{HD} = 0.18$ is far away from the final value of 1.05. This proves a kinetic hydrogen/deuterium isotope effect of the metathesis reaction. The determination of the kinetic isotope effects in a quantitative way was beyond the scope of this study. However, we estimate a kinetic isotope effect of about 5 at 77 K for reaction Eq. (3) as compared to Eq. (4).

3.4 *o*-H_2/*p*-H_2 Conversion and Isotope Scrambling of H_2/D_2 over Solid Vaska's Complex **1** at 77 K

In order to know whether the presence of the frozen organic solvent is essential to the *o-H₂/p-H₂* conversion and the isotope scrambling of H_2/D_2, we performed experiments with pure solid **1** under different conditions. For this purpose we loaded 150 mg (1.95×10^{-4} mol) of Vaska's complex **1** into the glass reactor depicted in Fig. 1 and cooled it to 77 K. Then we added either 400 mbar H_2 or 200 mbar H_2 and 200 mbar D_2 and let the gas interact with the solid at 77 K. A control experiment was performed at 298 K. After the exposure period the resulting gas mixture was brought into contact with a frozen standard solution of **1** in C_6D_6. Again, after thawing and careful shaking the sample the spectra depicted in Fig. 7 were taken.

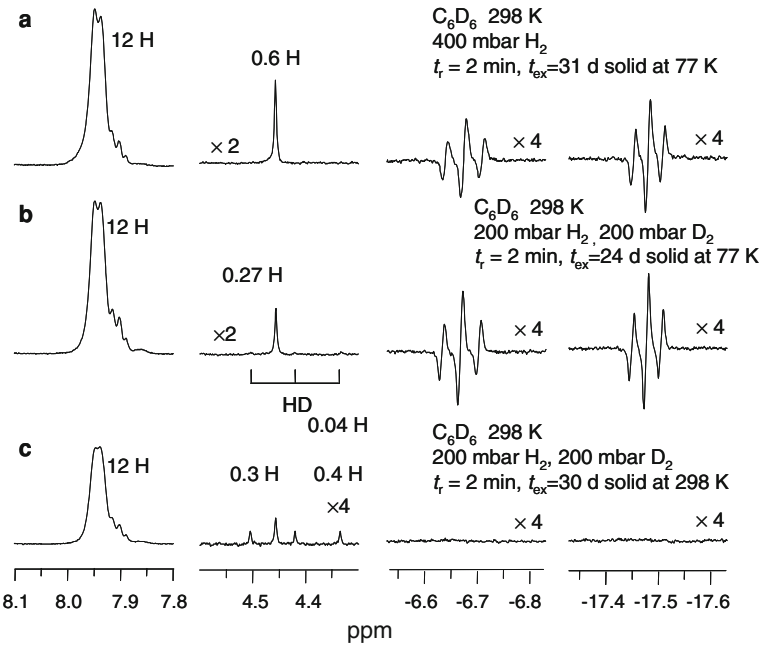

Fig. 7 ^{1}H NMR spectra at 298 K of standard samples of **1** in C_6D_6 under 400 mbar H_2 (**a**) and 200 mbar H_2 and 200 mbar D_2 (**b** and **c**) measured at time $t_r = 2$ min of the reaction to **2**. Prior to the addition of the solvent, the samples were exposed for different times t_{ex} at 77 K (**a** and **b**) and at 298 (**c**) to the warm dihydrogen gas mixture. Finally, 1 ml of solvent was added by vacuum transfer. (500.13 MHz, 4 scans, 20 s pulse delay, $\pi/4$ pulses 3.5 μs)

Figure 7a shows the spectrum of the first sample, where 400 mbar H_2 was let to interact with solid **1** at 77 K for 31 days. The spectrum is similar to those where benzene was present (Fig. 4). *p*-H_2 is clearly formed as illustrated by the observation of the PHIP signals at high field. The intensity of the dihydrogen signal was 0.6 H as compared to the signal of the aromatic *ortho*-phenyl protons exhibiting the intensity 12 H.

We repeated the same experiment with a mixture of 200 mbar of H_2 and a 200 mbar of D_2. Unfortunately, for experimental reasons, we could not let the gas mixture interact with **1** at 77 K only for 24 days. The results are depicted in Fig. 7b. As expected, again PHIP is observed indicating the formation of *p*-H_2. The dihydrogen signal intensity is about half of the one in Fig. 7a. Again we observe a small amount of HD, confirming the occurrence of the isotope scrambling reaction. However, in thermal equilibrium, we would expect a signal intensity of about 0.45 H, but we observe only a value of about 0.04 H indicating the presence of a kinetic isotope effect upon the oxidative addition.

In order to provide a reference for this finding, we performed an experiment where a 1:1 H_2/D_2 gas mixture was let to react with polycrystalline solid **1** for 30 days at 298 K. Of course no *para*-hydrogen enrichment could take place at RT and therefore no PHIP effect was observable. In the case where the equilibrium of the isotope scrambling is reached the HD signal intensity is expected to be

$$K = \frac{n_{\mathrm{HD}}{}^2}{n_{\mathrm{H2}}{}^2} \rightarrow \frac{n_{\mathrm{HD}}}{n_{\mathrm{H2}}} = \sqrt{3.25} = 1.8 = \frac{I_{\mathrm{HD}}}{I_{\mathrm{H2}}/2} = \frac{2I_{\mathrm{HD}}}{I_{\mathrm{H2}}} \rightarrow \frac{I_{\mathrm{HD}}}{I_{\mathrm{H2}}} = 0.9.$$

Here, we found a slightly larger value of 1.3, but the origin of the difference to the expected value was not further elucidated.

Although a quantitative determination of the relative rates of both processes was beyond the scope of this study, we can conclude already that a substantial part of *p*-H_2 is generated in the solid state by the *chemical SC*, rather than by *magnetic SC*. This result was surprising for us because *magnetic SC* requires a strong interaction of only one dihydrogen molecule with a transition metal catalyst, whereas for *chemical SC* at least two dihydrogen molecules are required.

Finally, we mention that a polycrystalline powder of **1** also catalyzes the heterogeneous hydrogenation of ethene in a gaseous 1:2 mixture (300 mbar C_2H_4 and 600 mbar H_2, 298 K) with ethane as gaseous product [17]. When a similar reaction is performed with styrene, the gaseous reaction product ethylbenzenepropene exhibits PHIP [7].

3.5 Dihydrogen in Frozen C_6D_6 in the Absence of Vaska's Catalyst

In order to understand how the *o*-H_2/*p*-H_2 conversion is catalyzed by Vaska's catalyst **1** in the cold solid state, we performed the following experiments. Firstly, we wanted to know what happens to the liquid solution when it is suddenly frozen. In order to study this question we performed the following experiment using an optical microscope. A standard solution of **1** in benzene was prepared, cooled to 77 K and exposed to 800 mbar of H_2. The sample was then thawed to room

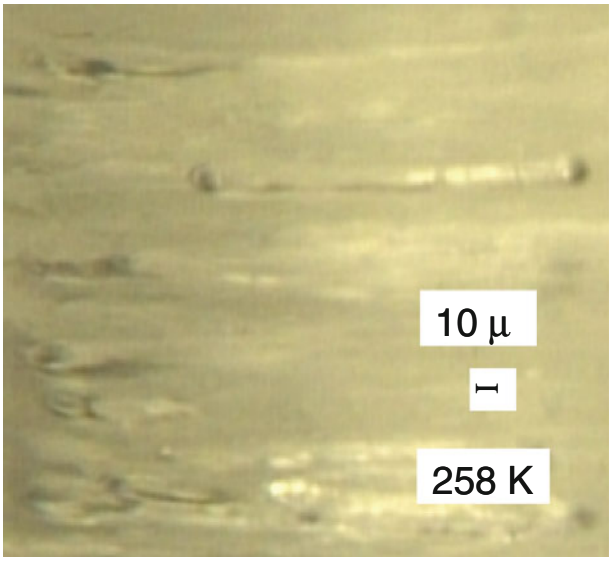

Fig. 8 Microscopic picture of a frozen solution of $Ir(CO)(Cl)(PPh_3)_2$ (**1**) in benzene

temperature, and cooled again to 258 K under the microscope. Near the freezing point of benzene at 278 K the sample solidified, releasing some dissolved dihydrogen. A picture of the frozen solid taken at 258 K is shown in Fig. 8. An irregular pore structure is observed as well as dark spots which we assign to small crystallites of **1**. Apparently, during the solidification a phase separation of solute and solvent takes place.

In the next step we had a look at H_2 in frozen C_6D_6 using low-temperature ^1H NMR. We would have liked to study the sample at liquid nitrogen temperature, but our setup allowed us only to go to about 100 K. For convenience, we performed the measurements at 110 K. Some spectra are depicted in Fig. 9. In order to compare the signal intensities all spectra were taken using the same number of scans, pulse lengths and waiting times. In addition, during Fourier transform they were referenced to each other.

Figure 9a shows the ^1H NMR spectrum of gaseous H_2 at room temperature. The usual broad signal around 4.5 ppm is observed, where the large line width of about 1,200 Hz is mainly caused by a short T_2 arising from dipolar and spin rotation relaxation [26].

For comparison, Fig. 9b depicts the ^1H spectrum of a thoroughly degassed standard sample of frozen benzene-d_6 (1 ml) prepared as described above, to which 800 mbar of H_2 were added at 77 K and then rapidly transferred to the NMR spectrometer pre-cooled to 110 K. We observe again a single signal at 4.5 ppm. The chemical shift and the line width are the same as for the gas phase, only the signal intensity is much smaller for H_2 in the frozen sample because the quantity of dihydrogen in the NMR coil is strongly reduced as frozen benzene is occupying most of the space. Therefore, we assign the signal in Fig. 9b to gaseous H_2 within pores formed in the frozen sample.

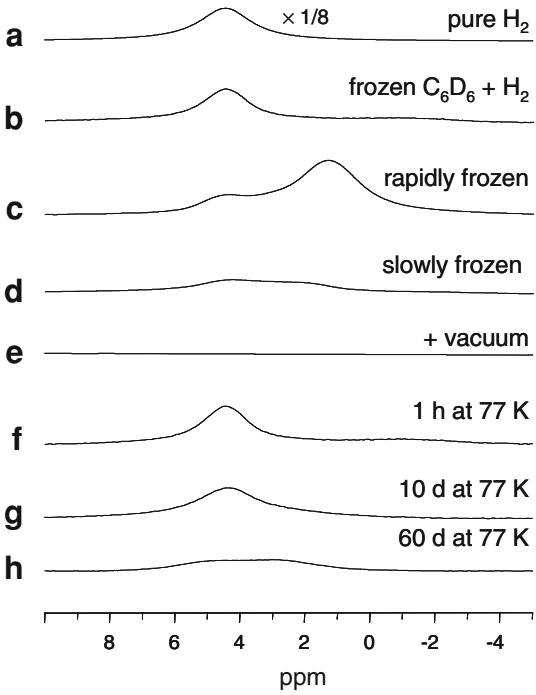

Fig. 9 ^{1}H NMR spectra of H_2 at 110 K. **a** 800 mbar in the gas phase. **b** After adding 800 mbar H_2 to a frozen sample (1 ml, 77 K) of C_6D_6 in a J. Young NMR tube and warming up to 110 K. **c** After warming the same sample to room temperature and fast cooling to 110 K. **d** After warming the same sample to room temperature and slow cooling to 77 K, then warming up to 110 K. **e** After connecting the frozen sample (77 K) to a vacuum line for 5 min at 10^{-6} mbar. **f** After adding again gaseous 800 mbar H_2 to the frozen C_6D_6 sample. **g** After 10 days at 77 K. **h** After 60 days at 77 K during which the sample was never thawed. Experimental conditions: 500 scans, 50 ms pulse delay, 12 μs pulse length, acquisition time 50 ms, constant receiver gain

Next, we thawed the sample thoroughly to room temperature, let the dihydrogen distribution between gas phase and solution equilibrate, and cooled the sample again rapidly to 110 K. The spectrum obtained is depicted in Fig. 9c. Now, in addition to the 4.5-ppm signal, an additional broad signal is observed at 1.2 ppm. We assign this signal to H_2 inside solid benzene. When the sample is cooled slowly, this signal is much smaller as illustrated in Fig. 9d.

We then cooled the NMR sample to 77 K and attached it to the vacuum line for 5 min at 10^{-6} mbar at 77 K, put it back into the spectrometer pre-cooled to 110 K, after which we obtained the spectrum depicted in Fig. 9e. We observed that all dihydrogen was now removed from the sample.

When H_2 was added again to this sample kept at 77 K without thawing, the spectrum shown in Fig. 9f was obtained showing only gaseous dihydrogen, as in the case of Fig. 9b. When this sample was kept at 77 K and measured again after 10 and 31 days at 110 K (Fig. 9g, h), very slowly the high-field signal came back.

These experiments show that dihydrogen is mobile in frozen benzene, and that there are two environments, i.e., large pores with gaseous dihydrogen, and dihydrogen inside the benzene phase.

3.6 Dihydrogen in Frozen C_6D_6 in the Presence of Vaska's Catalyst

In order to elucidate the interaction of dihydrogen with Vaska's catalyst in frozen benzene, we examined a standard sample of **1** in C_6D_6 at 110 K and 800 mbar by ^{1}H

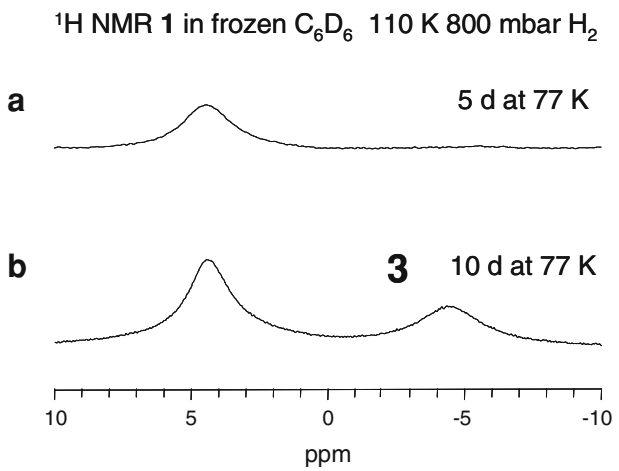

Fig. 10 ^{1}H NMR spectra of dihydrogen in frozen solutions of Ir(CO)(Cl)(PPh_3)$_2$ (**1**) in frozen C_6D_6 at 110 K. **a** After t_{ex} = 5 days of storage at 77 K. (**b**) After t_{ex} = 10 days of storage at 77 K

NMR. For that purpose, 800 mbar H_2 were added to the frozen solution at 77 K and stored at this temperature for 10 days. ^{1}H NMR spectra were taken after 5 and 10 days; and hence the sample was rapidly transferred to the NMR probe pre-cooled to 110 K.

The results are depicted in Fig. 10. After 5 days storage at 77 K only the signal for gaseous H_2 in large pores is observed, in agreement with the results depicted above in Fig. 9. However, after 10 days a new signal was observed at −4.5 ppm, but some signal intensity is left between 1 and 3 ppm. In Scheme 2 we propose an assignment for the high-field signal in terms of a η^2-dihydrogen complex **3** with Ir in the surface of a crystallite, taking into account that in that state the ligands cannot rearrange. Thus, either a very loose complex is formed, but it would also be possible that binding occurs to Ir in a defect which has lost a phosphine ligand as illustrated by structure **4**. Chemical shifts of η^2 dihydrogen bound Ru or Ir complexes can be anywhere between 0 and −50 ppm [27–31]. The relatively sharp signal in Fig. 10 indicates a high mobility of the dihydrogen moiety; thus, it is conceivable that there is a fast local exchange as illustrated in Scheme 2.

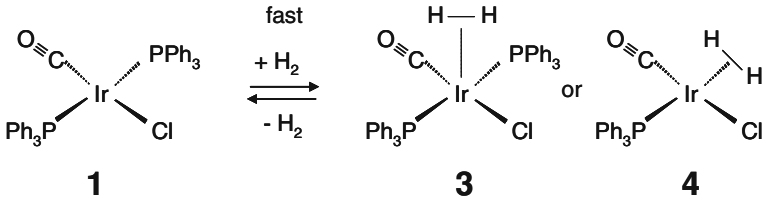

Scheme 2 Signal assignment referring to Fig. 10

4 Discussion

We have followed the reaction path of the *o*/*p*-H_2 spin conversion (SC) catalyzed by Vaska's complex **1** in frozen benzene and in the solid polycrystalline state using high-resolution ^{1}H NMR. During the conversion depicted in Scheme 1a, **1** does react to the dihydride **2** which was surprising for us initially. This reaction only takes place within 1 h in solution, and was used to detect the *p*-H_2 formed at low temperatures, as **2** exhibits PHIP. The PHIP signal intensity at 298 K is shown to be proportional to deviation of the *p*-H_2 concentration from the statistical value of 25 %. The catalyst does not only catalyze the *o*/*p*-H_2 spin conversion, but also catalyzes the isotope scrambling (IS) reaction Eq. (4) where H_2 and D_2 react to HD. Although the kinetic isotope effects could not be determined, we find qualitatively a large effect which is worthy of study in the future in a more quantitative way. One can conclude that also the *o*/*p*-H_2 spin conversion follows this chemical-SC pathway of Eq. (3) which requires that two dihydrogen molecules react after binding to Ir in the crystallite surfaces. The kinetic isotope effects could be interpreted in two ways. Either, there is a usual kinetic isotope effect arising from zero-point energy losses in the transition state. Or, there is no traditional kinetic isotope effect, but the *o*/*p*-H_2 spin conversion is faster than the isotope scrambling reaction because of an additional pathway via the magnetic-SC of Eq. (2). However, the latter is unlikely as it requires a strong reduction of the *o*/*p*-energy difference by binding of dihydrogen to the transition metal and an increase of the H···H distance, as shown previously [10, 11]. Such a binding, requires, however, a rearrangement of the ligands around Ir, a phenomenon which is suppressed in the solid state.

Before we discuss the chemical-SC in more detail, let us firstly interpret how Vaska's complex can catalyze the *o*/*p*-H_2 spin conversion at 77 K, which has been the original question of this work as described in Sect. 1.

In Fig. 11 a schematic microscopic scenario of the reaction is shown which is based on the microscopic and NMR studies described in the previous section. Dihydrogen gas molecules can enter from the warm gas phase the cold frozen benzene through cracks and pores. It can diffuse slowly through the entire solid, as it leaves the latter when the sample is exposed to a vacuum. Dihydrogen inside the pores exhibit similar chemical shifts as in the gas phase, around 4.5 ppm. However, dihydrogen can also be sandwiched between benzene molecules and resonate around 1 ppm, keeping their molecule mobility by diffusion through vacant or interstitial sites. Finally, they can bind to the surface of islands of Vaska's complex which has separated from the benzene during the freezing process. These islands can be quite small, leading to a surface area which is much larger than in a polycrystalline powder. This can explain why the *o*/*p*-H_2 spin conversion and the isotope scrambling reactions are faster in the frozen solutions as compared to the powder.

The spin conversion of *o*-H_2 to *p*-H_2 is catalyzed only in the cold area at 77 K by **1**. In this cold area, there is 50 % of both spin isomers in thermal equilibrium. That equilibrium is reached by the presence of the cold crystallites of **1** and by the many collisions of dihydrogen with the cold surfaces of **1** and of benzene. When some of the newly formed *p*-H_2 escapes the low-temperature region and goes back to the gas

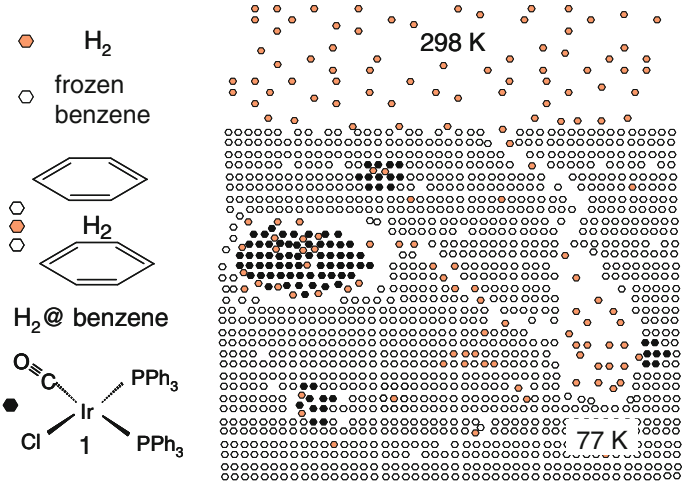

Fig. 11 Scenario of the interaction of dihydrogen with Vaska's complex **1**. For further information see text

phase above the cold solid it heats again to 298 K. However, as the spin conversion is very slow without catalyst, after long exposure times the spin temperature of dihydrogen in the gas phase is no longer the one at room temperature, but the one at 77 K.

Can our results tell us details about the chemical spin conversion and the isotope scrambling reaction at low temperatures which are unknown up to date? In the previous section we have provided some evidence for the formation of the dihydrogen complex **3**. As illustrated in Scheme 3, this complex might directly react with an additional dihydrogen molecule, in a similar way as was proposed by Noyori et al. [32] and by Morris et al. [33] for the case of hydrogenation of ketones by Ru-complexes. Such a configuration of type **5** might be stabilized by secondary interactions with chlorine as illustrated by structure in Scheme 3, as was proposed previously [17]. On the other hand, it might also be that both phosphine ligands leave Ir in solution, as has been discussed by Vaska et al. [18], leaving some very reactive Ir centers in the surfaces of the crystallites, which could react with two dihydrogen molecules to a configuration of type **6** in Scheme 3. Such a configuration could also be active for the observed hydrogenation of double bonds by polycrystalline **1** [17].

Evidence for binding of more than one dihydrogen molecule to Ir centers comes from the finding that polycrystalline **1** catalyzes the hydrogenation of ethene gas (300 mbar) by dihydrogen (600 mbar) at room temperature directly in a closed NMR tube (Scheme 4). Usually, this reaction takes place in solution and requires binding of one dihydrogen and one ethene molecule. Again, in the solid state it is conceivable that the reaction takes place in defect sites of crystal surfaces which are able to bind more than one molecule. The discovery that homogeneous hydrogenation catalysts might also work as heterogeneous catalysts has been confirmed by Koptyug et al. [6, 7] via gas-phase PHIP studies.

Scheme 3 Possible reactive configurations of the isotope scrambling reaction catalyzed by **1**

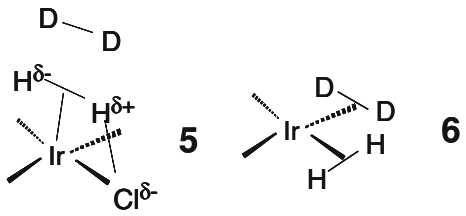

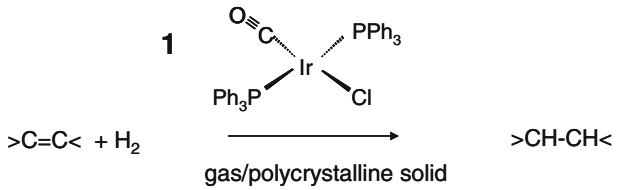

Scheme 4 Hydrogenation of ethene gas by polycrystalline **1** according to Ref. [17]

5 Conclusions

We conclude that exploring both the liquid and solid-state activity of a catalyst may help to bridge the gap between the homogeneous and heterogeneous catalysis and to provide additional information about the reaction mechanisms. Here, we have obtained some evidence for a dihydrogen complex as intermediate species of the formation of Vaska's dihydride **2** by oxidative addition of dihydrogen to Vaska's complex **1** (Scheme 1). Moreover, a consistent picture of the accidental finding of the production of *p*-H_2 by Eisenberg et al. [1, 2] has been provided. The observation that the reaction is faster in frozen solutions of **1** as compared to polycrystalline **1** can be explained in terms of the presence of smaller particles exhibiting a larger surface area. An unsolved problem is the details of the structure of the active reaction centers. It could not be elucidated whether each Ir complex in the surface can react or whether only defects are reactive which have lost one or even two ligands, allowing binding of two dihydrogen molecules. We hope that we will make progress in this field using solid-state ^{2}H NMR spectroscopy which is able to characterize the type of deuterium binding to transition metals as well as their dynamics [34–38].

Acknowledgments We thank the Deutsche Forschungsgemeinschaft Bonn (contract Bu-911-15-1) for financial support.

References

1. T.C. Eisenschmid, R.U. Kirss, P.P. Deutsch, S.I. Hommeltoft, R. Eisenberg, J. Bargon, R.G. Lawler, A.L. Balch, J. Am. Chem. Soc. **109**, 8089–8091 (1987)
2. R. Eisenberg, Acc. Chem. Res. **24**, 110–116 (1991)
3. C.R. Bowers, D.P. Weitekamp, J. Am. Chem. Soc. **109**, 5541–5542 (1987)
4. S.E. Korchak, K.L. Ivanov, A.V. Yurkovskaya, H.-M. Vieth, Phys. Chem. Chem. Phys. **11**, 11146–11156 (2009)

5. M. Haake, J. Natterer, J. Bargon, J. Am. Chem. Soc. **118**, 8688–8691 (1996)
6. L.S. Bouchard, K.V. Kovtunov, S.R. Burt, M.S. Anwar, I.V. Koptyug, R.Z. Sagdeev, A. Pines, Ang. Chem. Int. Ed. **46**, 4064–4068 (2007)
7. I.V. Koptyug, K.V. Kovtunov, S.R. Burt, M.S. Anwar, C. Hilty, S.I. Han, A. Pines, R.Z. Sagdeev, J. Am. Chem. Soc. **129**, 5580–5586 (2007)
8. R.W. Adams, J.A. Aguilar, K.D. Atkinson, M.J. Cowley, I.P.P. Elliott, S.B. Duckett, G.G.R. Green, I.G. Khazal, J. Lopez-Serrano, D.C. Williamson, Science **323**, 1708–1711 (2009)
9. G. Buntkowsky, J. Bargon, H.H. Limbach, J. Am. Chem. Soc. **118**, 8677–8683 (1996)
10. H.H. Limbach, G. Buntkowsky, J. Matthes, S. Gründemann, T. Pery, B. Walaszek, B. Chaudret, Chem. Phys. Chem. **7**, 551–554 (2006)
11. G. Buntkowsky, B. Walaszek, A. Adamczyk, Y. Xu, H.H. Limbach, B. Chaudret, Phys. Chem. Chem. Phys. **8**, 1929–1935 (2006)
12. G.J. Kubas, R.R. Ryan, B.I. Swanson, P.J. Vergamini, H. Wassermann, J. Am. Chem. Soc. **106**, 451–452 (1984)
13. G.J. Kubas, Acc. Chem. Res. **21**, 120–128 (1988)
14. H.H. Limbach, G. Scherer, M. Maurer, B. Chaudret, Angew. Chem. Int. Ed. **31**, 1369–1372 (1992)
15. H.H. Limbach, S. Ulrich, G. Buntkowsky, S. Gründemann, S. Sabo-Etienne, B. Chaudret, G.J. Kubas, J. Eckert, J. Am. Chem. Soc. **120**, 7929–7943 (1998)
16. S. Gründemann, H.H. Limbach, V. Rodriguez, B. Donnadieu, S. Sabo-Etienne, B. Chaudret, Ber. Bunsenges. Phys. Chem. **102**, 344–353 (1998)
17. J. Matthes, T. Pery, S. Gründemann, G. Buntkowsky, S. Sabo-Etienne, B. Chaudret, H.H. Limbach, J. Am. Chem. Soc. **126**, 8366–8367 (2004)
18. M.E. Tadros, L.J. Vaska, Colloid Interfac. Sci. **85**, 389–410 (1982)
19. L.J. Vaska, Acc. Chem. Res. **1**, 335–344 (1968)
20. B.A. Messerle, C.J. Sleigh, M.G. Partridge, S.B. Duckett, J. Chem. Soc., Dalton Trans. 1429–1436 (1999). http://www.crossref.org/guestquery/
21. S.K. Hasnip, S.B. Duckett, C.J. Sleigh, D.R. Taylor, G.K. Barlow, M.J. Taylor, Chem. Commun. 1717–1718 (1999). http://www.crossref.org/guestquery/
22. P.B. Chock, J.J. Halpern, J. Am. Chem. Soc. **88**, 3511–3514 (1966)
23. I.F. Silvera, Rev. Mod. Phys. **52**, 393–452 (1980)
24. H.C. Urey, J. Chem. Soc. 562–581 (1947)
25. O. Thompson, O.A. Schaeffer, J. Chem. Phys. **23**, 759–760 (1955)
26. A. Abragam, *The Principles of Nuclear Magnetism* (Clarendon Press, Oxford, 1961)
27. V. Rodriguez, S. Sabo-Etienne, B. Chaudret, J. Thoburn, S. Ulrich, H.H. Limbach, J. Eckert, J.C. Barthelat, K. Hussein, C.J. Marsden, Inorg. Chem. **37**, 3475–3485 (1998)
28. J. Matthes, S. Gründemann, A. Toner, Y. Guari, B. Donnadieu, S. Sabo-Etienne, E. Clot, H.H. Limbach, B. Chaudret, Organometallics **23**, 1424–1433 (2004)
29. V. Pons, D.M. Heinekey, J. Am. Chem. Soc. **125**, 8428–8429 (2003)
30. M. Findlater, K.M. Schultz, W.H. Bernskoetter, A. Cartwright-Sykes, D.M. Heinekey, M. Brookhart, Inorg. Chem. **51**, 4672–4678 (2012)
31. P. Mura, J. Coord. Chem. **51**, 253–260 (2000)
32. M. Yamakawa, H. Ito, R. Noyori, J. Am. Chem. Soc. **122**, 1466–1478 (2000)
33. K. Abdur-Rashid, A.J. Lough, R.H. Morris, Organometallics **19**, 2655–2657 (2000)
34. B. Walaszek, A. Adamczyk, T. Pery, Y. Xu, T. Gutmann, N. Amadeu de Sousa, S. Ulrich, H. Breitzke, H.-M. Vieth, S. Sabo-Etienne, B. Chaudret, H.H. Limbach, G. Buntkowsky, J. Am. Chem. Soc. **130**, 17502–17508 (2008)
35. G. Buntkowsky, H.H. Limbach, B. Walaszek, A. Adamczyk, Y. Xu, H. Breitzke, A. Schweitzer, T. Gutmann, M. Wächtler, N. Amadeu, D. Tietze, B. Chaudret, Z. Phys. Chem. **222**, 1049–1064 (2008)
36. T. Gutmann, B. Walaszek, Y. Xu, M. Wächtler, A. Grünberg, I. del Rosal, R. Poteau, R. Axet, G. Lavigne, B. Chaudret, H.H. Limbach, G. Buntkowsky, J. Am. Chem. Soc. **132**, 11759–11767 (2010)
37. S. Macholl, J. Matthes, H.H. Limbach, S. Sabo-Etienne, B. Chaudret, G. Buntkowsky, Solid State NMR **36**, 137–143 (2009)
38. I. del Rosa, T. Gutman, B. Walaszek, I.C. Gerber, B. Chaudret, H.H. Limbach, G. Buntkowsky, R. Poteau, Phys. Chem. Chem. Phys. **13**, 20199–20207 (2011)